Extremely long Kelvin-Helmholtz billow trains in the Romanche Fracture Zone

Hans van Haren, Louis Gostiaux, Eugene Morozov, Roman Tarakanov

Geophysical Research Letters

AN AGU JOURNAL

Volume 41 • Issue 23 • 16 December 2014 • Pages 8147–8672

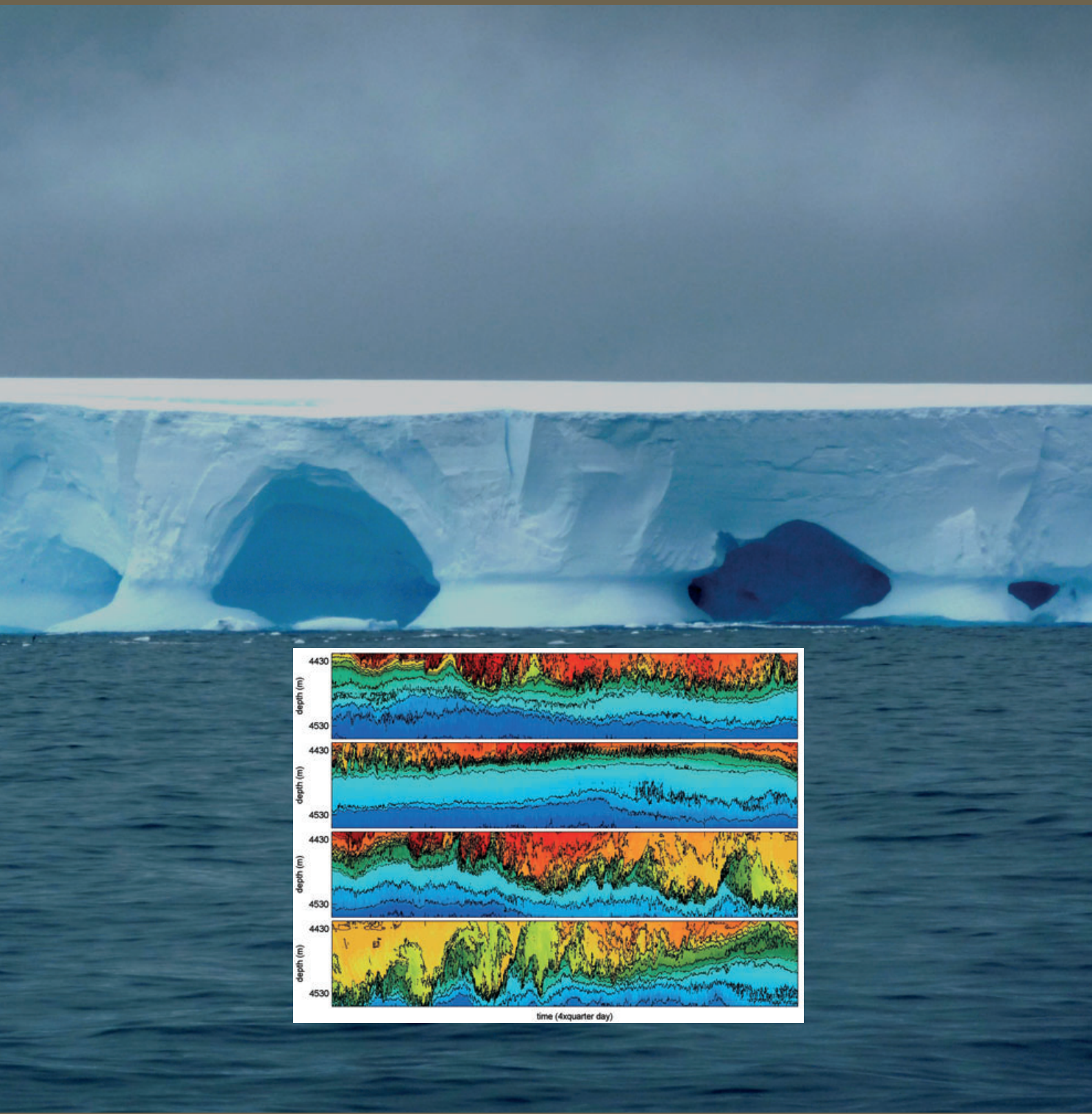

AGU PUBLICATIONS

WILEY

AGU PUBLICATIONS

Geophysical Research Letters

RESEARCH LETTER
10.1002/2014GL062421

Key Points:
- Long train of Kelvin-Helmholtz billows
- Details of shear-induced turbulence
- Rapid warming of Antarctic Bottom Water just past its entrance in RFZ

Correspondence to:
H. van Haren,
hans.van.haren@nioz.nl

Citation:
van Haren, H., L. Gostiaux, E. Morozov, and R. Tarakanov (2014), Extremely long Kelvin-Helmholtz billow trains in the Romanche Fracture Zone, *Geophys. Res. Lett.*, *41*, 8445–8451, doi:10.1002/2014GL062421.

Received 3 NOV 2014
Accepted 16 NOV 2014
Accepted article online 18 NOV 2014
Published online 9 DEC 2014

Extremely long Kelvin-Helmholtz billow trains in the Romanche Fracture Zone

Hans van Haren[1], Louis Gostiaux[2], Eugene Morozov[3], and Roman Tarakanov[3]

[1]NIOZ Royal Netherlands Institute for Sea Research, Den Burg, Netherlands, [2]Laboratoire de Mécanique des Fluides et d'Acoustique, École Centrale de Lyon, Université de Lyon, Écully, France, [3]Shirshov Institute of Oceanology, Russian Academy of Sciences, Moscow, Russia

Abstract In the Atlantic Ocean, the densest water mass Antarctic Bottom Water "AABW" can only cross the Mid-Atlantic Ridge from its southwestern to northeastern basins in limited, because deep, conduits. At the southwestern entrance of one of these, the equatorial Romanche Fracture Zone, AABW crosses a sill at 4550 m depth in a 7 km narrow channel before plunging into the deep. At the sill-slope, the rapidly flowing AABW causes shear-induced turbulent mixing with the overlying water masses. We present an excerpt of 1 Hz sampled, half-yearlong moored observations from 99 high-resolution temperature sensors that demonstrate and quantify the turbulence details. On top of quasi-steady shear flow, an internal tide modulates the mixing. Together, they constitute a means for an extremely long train of >250 consecutive Kelvin-Helmholtz billows in a day that vary between 5 and 100 m in vertical scale.

1. Introduction

The Romanche Fracture Zone (RFZ) is one of three main pathways for Antarctic Bottom Water (AABW) propagation from the western to the eastern Atlantic [*Morozov et al.*, 2010]. Just before AABW enters the RFZ at 22°30′W its conservative temperature is about $\Theta = 0.5$°C; it is 0.65°C within the fracture at 22°10′W (2011 data) [*Tarakanov et al.*, 2013]. After the exit from the RFZ to the Sierra Leone Basin at 13°W it is 1.66°C [*Mantyla and Reid*, 1983]. The considerable warming of AABW during the passage through the RFZ is attributed to strong mixing with overlying Atlantic waters ($\Theta > 1.9$°C) [*Mercier and Morin*, 1997]. This mixing has previously been found over the sills near the RFZ exit [*Polzin et al.*, 1996; *Ferron et al.*, 1998; *Mercier and Speer*, 1998]. Recently, equally strong mixing, with mean eddy diffusivity values of $K_z = O(10^{-2})$ m^2 s^{-1}, was reported near the southwestern entrance of RFZ [*Tarakanov et al.*, 2013].

The precise knowledge of mixing near the RFZ entrance is important for correctly modeling its efficiency further along in the RFZ, as (initial) mixing modifies the stratification. It is also important for a better understanding of the role of narrow conduits in global ocean water mass transport models. The above mixing estimates have been based on shipborne profiler measurements. Such measurements do not explicitly reveal the mechanism of the mixing process itself. This process will be shown in the present paper using high-resolution moored observations.

The flow over the sill of the southwestern entrance creates a vertical current shear that is strongest around 200 m above the bottom (hereafter mab). In combination with the channel-like topography, the descending flow can thus provide an ideal environment for shear-induced turbulence generation of the Kelvin-Helmholtz billow "KHb" type. In laboratory experiments, under constant shear, a quasi-infinite train of KHb may be observed, limited only by the size of the apparatus [e.g., *Thorpe*, 1968]; see also numerical modeling results by *Scinocca and Ford* [2000]. In nature, observations of such long trains of KHb are rare [*Bacmeister and Schoeberl*, 1989; *Thorpe*, 2005; *Smyth and Moum*, 2012]. This may be because shear flows rarely persist over long enough spatial and temporal scales [e.g., *Wesson and Gregg*, 1994; *Farmer and Armi*, 1999].

Here we report the observation of an extremely long KHb train (containing >250 billows or overturns) and quantify various mixing processes of AABW with overlying North Atlantic waters.

2. Data and Methods

Between October 2013 and April 2014, a 350 m long deep-sea mooring was deployed in 4720 m water depth at 01°05.034′ S, 022°27.652′ W (Figure 1). The immediate surrounding topography has a depth of 3500–4000 m, so that the mooring reached to approximately halfway up in the 7 km wide meridional channel connecting RFZ and the fracture to the south.

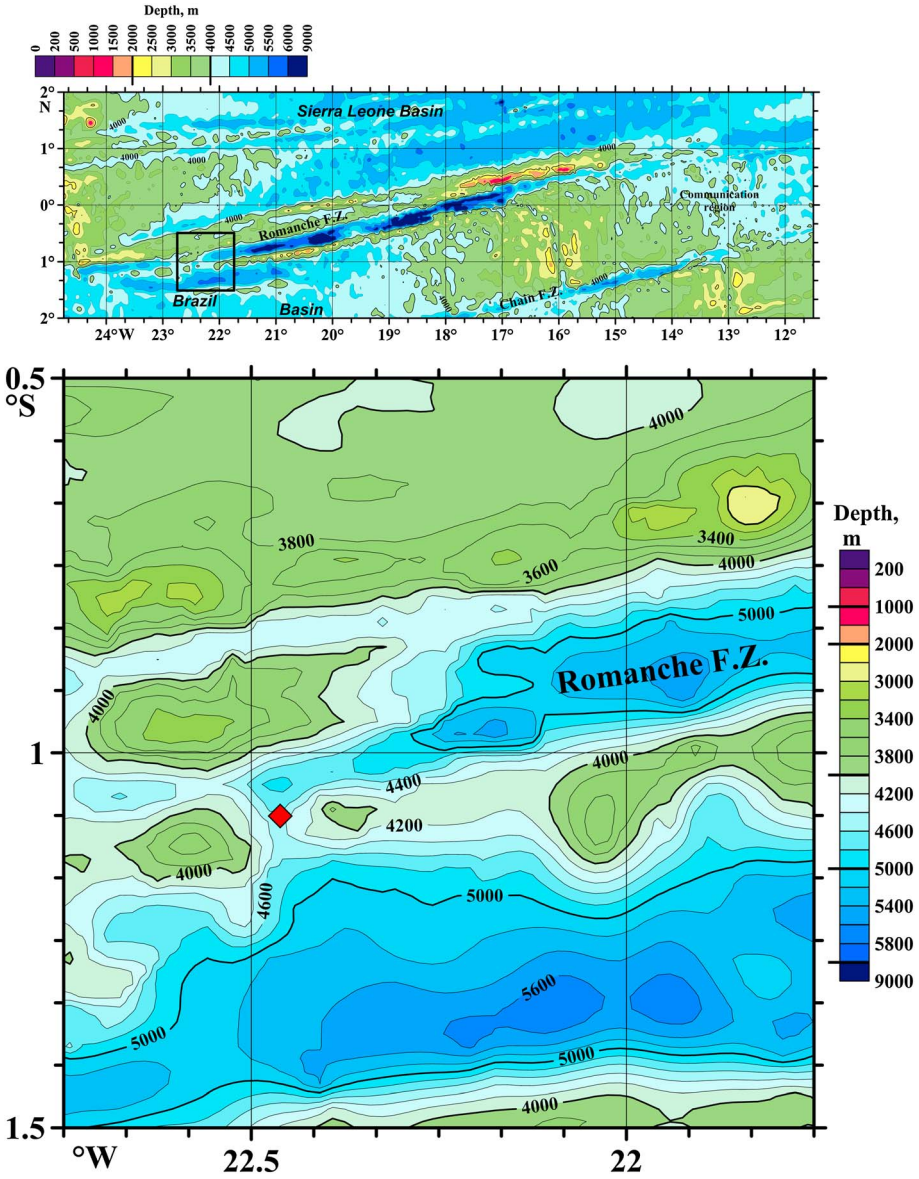

Figure 1. Mooring site (red diamond) in the southwestern entrance of the RFZ using ETOPO-1 data [*Smith and Sandwell*, 1997] and additional echosounder data.

The mooring had 200 kg net buoyancy. It held upright two Nortek AquaDopp acoustic current meters at 4414 and 4612 m and between those a 198 m long 0.007 m diameter nylon-coated steel cable to which every 2 m a NIOZ4 high-resolution temperature sensor was taped. Of the total of 99 sensors, 10 showed battery, electronics, or calibration problems. Their data were interpolated between those of the neighboring sensors. The current meters sampled at a rate of once per 600 s, the temperature sensors at 1 Hz with a time delay of <0.02 s as they were synchronized inductively every 4 h [*van Haren et al.*, 2009].

The low noise level of 6×10^{-5}°C permits to use these moored temperature observations to estimate stratified turbulence parameters like dissipation rate ε and K_z [*van Haren and Gostiaux*, 2012]. Thereby, the sorting method of unstable portions of a vertical density profile into a monotonic stable profile and, for these highly turbulent waters, a constant mixing efficiency of 0.2 is used [*Thorpe*, 1977; *Osborn*, 1980; *Dillon*, 1982]. The latter is a mean value for shear-induced turbulence in high Reynolds number flows, with variations over 1 order of magnitude [e.g., *Wesson and Gregg*, 1994; *Mashayek et al.*, 2013]. The contribution from salinity besides temperature to local density variations is established from repeated shipborne SeaBird 19+

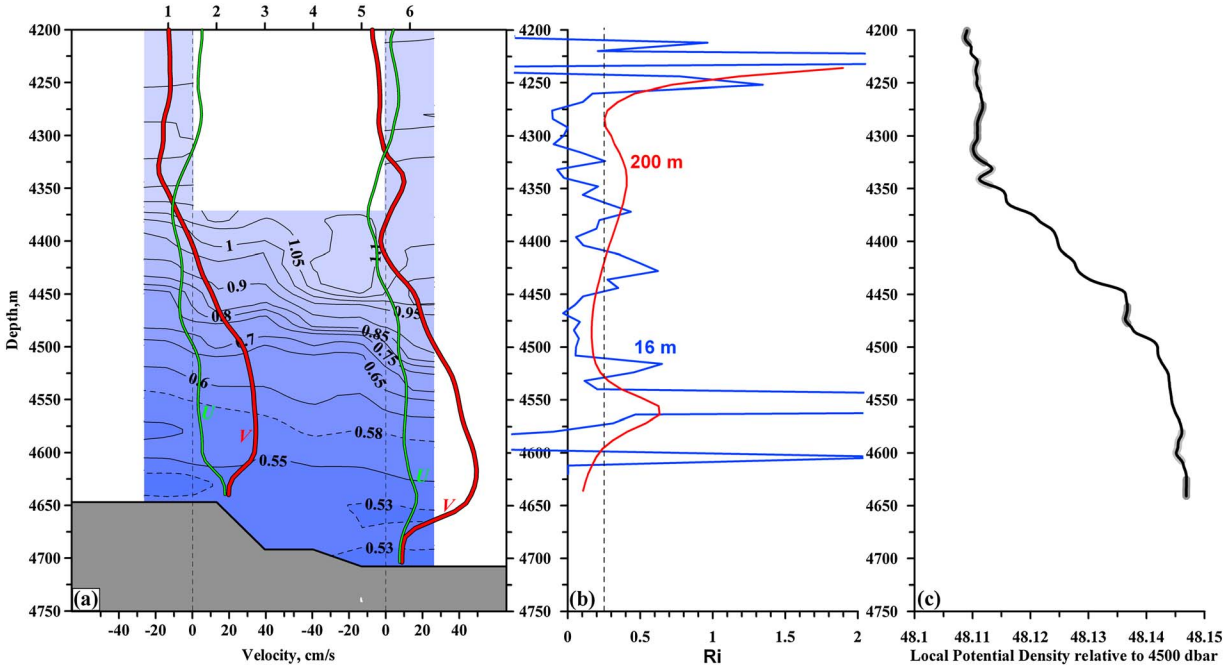

Figure 2. Vertical profiles of shipborne CTD/LADCP observations from the mooring deployment cruise in October 2013. (a) Current profiles and temperature contours. (b) Gradient Richardson number of raw 16 m data (blue) and smoothed over 200 m vertical intervals (red). The vertical dashed line indicates $Ri = 1/4$. (c) Potential density anomaly with reference to 4500 dBar. Density inversions are indicated by thick lines.

Conductivity-Temperature-Depth "CTD" profiles next to the mooring. Thus, the pressure-corrected conservative temperature [*McDougall et al.*, 2009] is related to density-anomaly variations referenced to 4000 m: $\delta\sigma_{4000} = \alpha\delta\Theta$, in which $\alpha = -0.091 \pm 0.001$ kg m^{-3}°C^{-1} denotes the apparent expansion coefficient. Turbulence parameter estimates are made over the entire 196 m vertical range of temperature sensors for every 1 Hz profile. Averaging over time is denoted by […] and averaging over depth by $<\ldots>$.

Besides CTD, lowered 300 kHz, 16 m binned TeleDyne/RDI-Acoustic Doppler Current Profiler "LADCP" profiles were obtained during mooring deployment and recovery cruises.

3. Observations

Vertical CTD/LADCP profiles demonstrate a 0.3–0.4 m s^{-1} northward flow between about 30 and 230 mab, the dense AABW plunges into the fracture (Figures 2a and 2c). The level of shear stability, as indicated by the gradient Richardson number $Ri = N^2/|\mathbf{S}|^2$ where N denotes the buoyancy frequency of stable stratification and $S = [dU/dz, dV/dz]$ the destabilizing shear vector for horizontal current components U (east-west) and V (north-south), is close to 0.25 (Figure 2b). This implies marginal linear stability [*Miles*, 1961; *Howard*, 1961]. This value varies with the internal tide, as is inferred from the moored observations. The negative Ri values in the original 16 m scale data reflect inversions due to overturns of the stable density profile (Figure 2c). Such inversions disappear when averaging with time is longer than the buoyancy period or when vertical smoothing is exceeding the largest overturn scale, >100 m here. The resulting marginal (in)stability has similar low Ri values as found in inertial shear with steady magnitude [*van Haren et al.*, 1999] and in the equatorial undercurrent [*Smyth and Moum*, 2013].

We deliberately focus on a 4 day long portion (Figure 3) that is characteristic for the entire half-year long observational record. Over the entire vertical range and during the entire data set, a typical cold temperature of AABW, the 0.85°C isotherm, color green-yellow here, is well-captured by the string of thermistors while it varies with the semidiurnal tide mainly over a range of up to 100 m (Figure 3a). Superposed on these are shorter-term variations. The 0.85°C isotherm is part of a rather sharp transition in density between the relatively warmer upper and cooler lower waters. Temperatures in both the lower ($\Theta = 0.5$–0.7°C) and upper

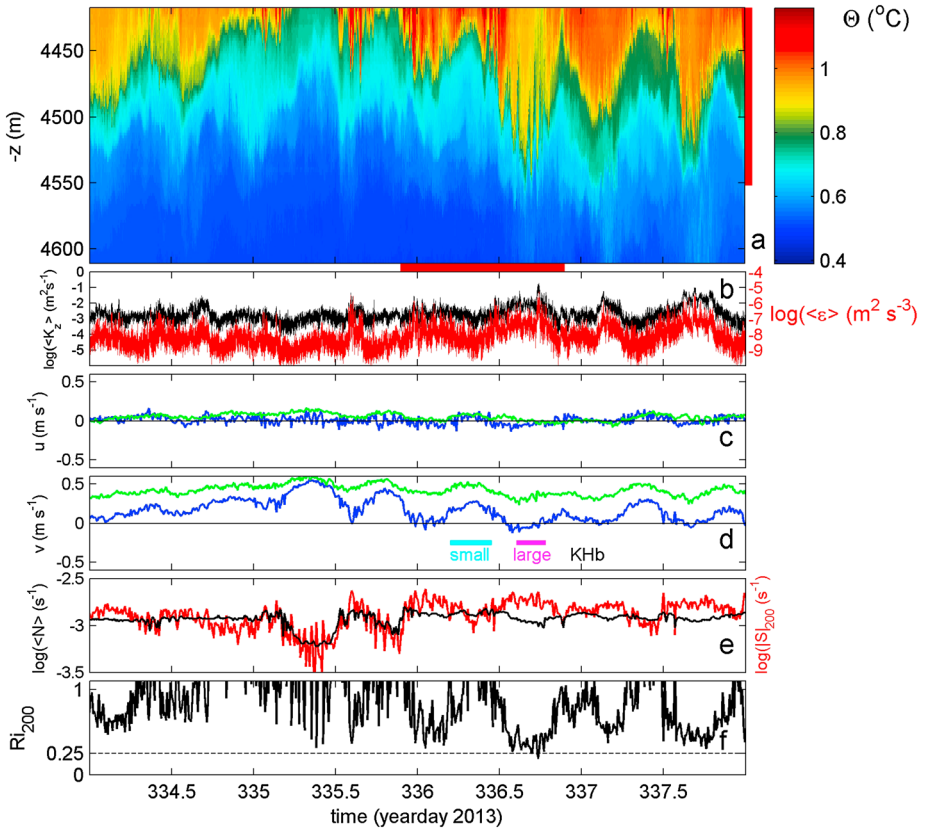

Figure 3. Four-day long sample of observations. (a) Depth-time series of 2 m and 1 Hz sampled conservative temperature Θ. The local bottom is 108 m below the lowest sensor. The horizontal red bar indicates the period of Figure 4, the vertical bar its depth range. (b) Time series of 196 m vertically averaged turbulence dissipation rate ε (red) and eddy diffusivity K_z (black) using the data of Figure 3a and a constant linear relationship between temperature and density variations (see section 2). (c) East (+)-west (−) current component, from upper (blue) and lower current meter (green). (d) As in Figure 3c but for the north (+)- south (−) current component. The period of a train of small-scale KHb is indicated by the light blue bar, that of large-scale KHb by the purple bar. (e) Buoyancy frequency and shear magnitude, computed over 200 m vertically. (f) *Ri* computed as the squared ratio of $<$N$>$ and $|\mathbf{S}|_{200}$ shown in Figure 3e.

(Θ = 1.0–1.2°C) layers vary in time. These variations in temperature within a particular layer imply active mixing between the waters above and below, followed by a rapid transport by the larger-scale currents.

Values of ε and K_z, averaged over the entire vertical range of temperature sensors, vary over 3–4 orders of magnitude (Figure 3b), with tidal variability peaking when the warm-overlying waters are deepest and the current speeds generally weakest (Figures 3c and 3d). The current, strongest near the bottom of the range, is predominantly directed northward, with a tidal modulation. Averages over the 4 day period of $[<\varepsilon>] = 2.4 \pm 1 \times 10^{-8}\ \mathrm{m^2\ s^{-3}}$ and $[<K_z>] = 4 \pm 2 \times 10^{-3}\ \mathrm{m^2\ s^{-1}}$ are half an order of magnitude lower than the estimates based on CTD/LADCP observations in the same area in 2011 [*Tarakanov et al*., 2013]. The presently observed values are more than 1 order of magnitude larger than the canonical value [*Munk and Wunsch*, 1998] needed to maintain the ocean stratified over its entire depth and about 2 orders of magnitude larger than open ocean values [*Gregg*, 1989; *Polzin et al*., 1996]. These values are observed in relatively strong stratification of $[<\mathrm{N}>] = 1.0 \pm 0.5 \times 10^{-3}\ \mathrm{s^{-1}}$, given the large depth, and which allows a mean small-scale internal wave period of down to $2\pi/[<\mathrm{N}>] = 6000$ s (0.07 days). The 200 m shear magnitude $|\mathbf{S}|_{200}$ computed as finite difference between current meter data shows a larger variation with time than $<$N$>$, with an in-phase tidal modulation (Figure 3e). It provides a large-scale $\mathrm{Ri}_{200} = <\mathrm{N}>^2/\mathbf{S}_{200}{}^2$ (Figure 3f), regularly between 0.25 and 1, that is marginally stable confirming CTD/LADCP data, when $<\varepsilon>$ and $<K_z>$ are (tidally) peaking.

High-frequency internal waves of periods of 0.07 days and longer are observed in the detail 1 day long image of temperature and stratification (Figure 4). (Turbulence parameter averages over this 1 day period

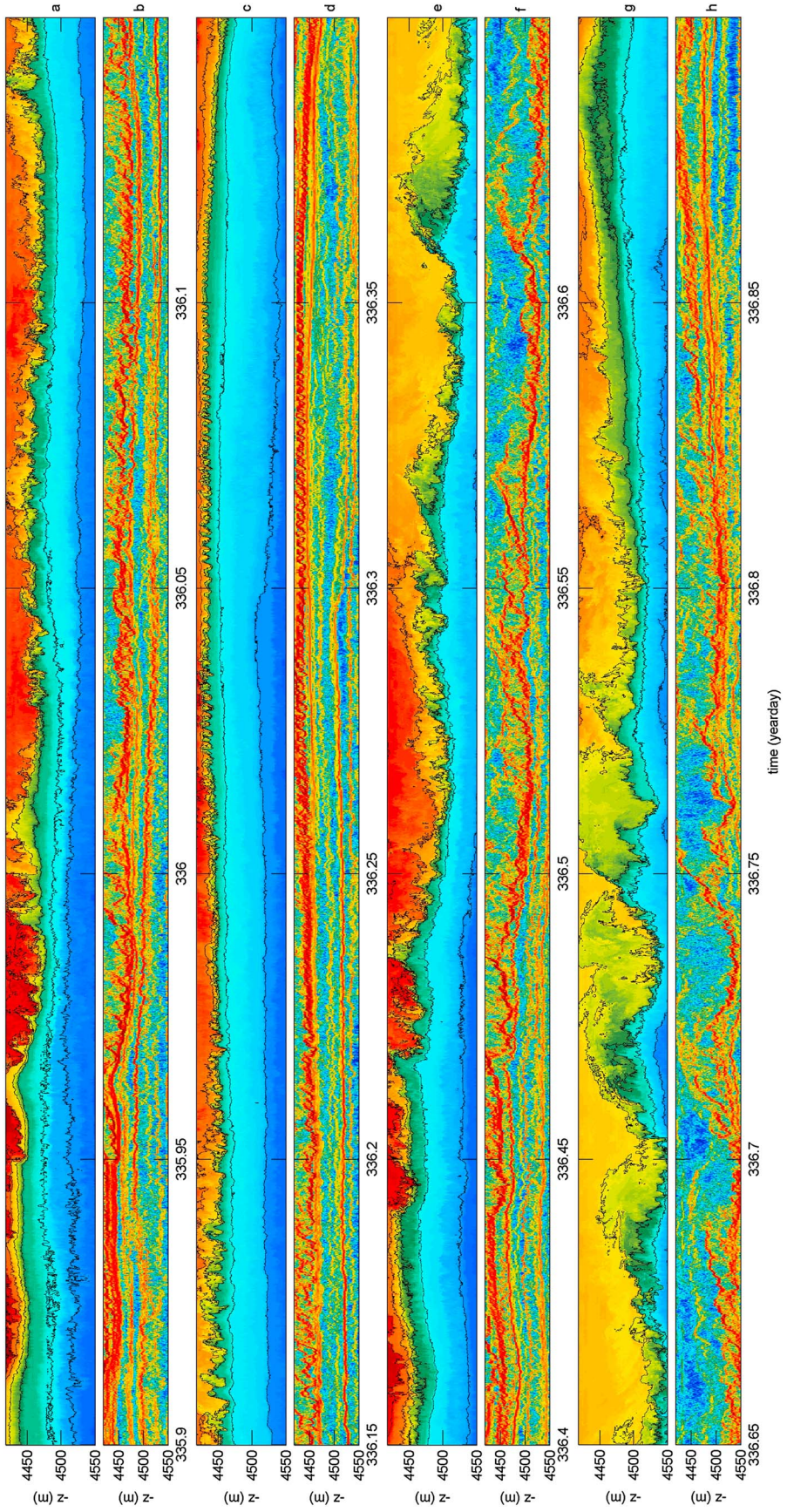

Figure 4. One day detail in four consecutive parts showing shear-induced overturning. (a, c, e, and g) Conservative temperature, with the same color scheme as in Figure 3a and contours every 0.1°C in black. (b, d, f, and h) Buoyancy frequency computed from the data in Figure 4a, sorted per time step in a statically stable profile. The color range [blue, red] is on a log-scale for $[-4, -2.4]$ (which corresponds to a linear range of $[10^{-4}, 4 \times 10^{-3}]$ s^{-1}).

are $[<\varepsilon>] = 4 \pm 2 \times 10^{-8}\,m^2\,s^{-3}$, $[<K_z>] = 6 \pm 3 \times 10^{-3}\,m^2\,s^{-1}$.) However, much more rapid motions catch the eye, especially also as particular characteristic s or eye shapes [*Geyer and Smith*, 1987; *Geyer et al*., 2010; *Fukao et al*., 2011] of thin-layer (orange-red) stratification. All the rapid variations are thus not freely propagating internal waves, but most likely turbulence, in particular KHb, with overturns advected in part by the horizontal currents passing the mooring site.

In this particularly rich sample of overturns, we counted an uninterrupted sequence of 275 ± 25 KHb. These KHb vary from an extensive train of 5–10 m small ones, passing between days 336.2 and 336.45 when large-scale $Ri \approx 1$ (Figure 3f), to a sequence of up to 100 m overturns, between days 336.61 and 336.78 when large-scale $Ri \approx 0.3$. The large change in amplitude and length of billows from one tidal cycle to the next suggests an increase in the thickness of the transitional layer due to a change in the internal tide/large-scale current interaction or to another, unknown process occurring upstream. The sensor separation of 2 m also resolves smaller-scale secondary KHb superposed on the rims of the latter [*Corcos and Sherman*, 1976], best viewed in the stratification data. The KHb activity is thus intense that the braid transition between individual overturns is relatively small to the stage of near merging. Yet merging is not occurring and the saturated billows remain stable, creating a long train of billows.

4. Conclusions

The uninterrupted train of KHb shown in Figure 4 is, to our knowledge, the longest observed in either the ocean or the atmosphere. Long KHb trains point at a rather persistent low stability of the stratified environment. Such marginal stability in terms of *Ri* across an intense "thin-layer" stratification can only be achieved by a strong shear persistent in time. In the present case, the channel shape of the southwestern RFZ entrance sets up a continual flow of ~0.25 m s^{-1} in the lower 100–200 mab. This flow creates the background shear necessary to maintain small-scale overturning stability even if the tidal current is in the opposing direction. During the phase when the tidal current is directed opposite to the steady northward flow, the shear is largest and the 100 m large overturns are observed. The long train of 5–10 m small KHb is found under moderate shear, during the phase when the tidal current is with the steady flow. No other flows contribute sufficiently to maintain the stratification marginally stable. Thus, long KHb trains are observed, instead of the commonly 3–10 KHb trains that are much like the sequence of the 100 m large ones here. This train of large consecutive KHb is observed to contain small-scale, secondary KHb in the braids along the thin interfaces around and between them, e.g., day 336.15 around 4450 m, except for a weaker stratified "gap" on one side of the KHb, e.g., day 336.7 around 4480 m. This also occurs in high Reynolds number estuarine flows, following detailed acoustic observations [*Geyer et al*., 2010] that reflect the stratification images here.

The implication is highly effective mixing along the thin-layer stratified border of the large overturns [*Corcos and Sherman*, 1976], with an opening to actively turbulent large overturning on the opposing side. Although the present observations were made at large depths >4000 m, their environment is nearly as turbulent as an estuarine environment, with mean eddy diffusivity values O(10^{-2}) m^2 s^{-1} and turbulence dissipation rates O(10^{-8} m^2 s^{-3}). The strong turbulence conditions are manifest in the braids bordering large-scale billows. These are only observed in very active shear and high Reynolds number conditions. It appears that this turbulent mixing mechanism is the main cause for the rapid warming of AABW during its passage over sills through the RFZ, with an important role for the sill in the southwestern entrance studied here.

Acknowledgments

We thank the crew of the R/V *Ak*. S. Vavilov for deployment and recovery of the mooring. We are grateful to Martin Laan for all his "thermistor-support." The research cruises were financed by Program 23 of the Presidium of the Russian Academy of Sciences and the Russian Foundation for Basic Research. The paper was initiated during HvH's stay as a visiting professor at and financed by the École Centrale de Lyon. L.G. supported by the Agence Nationale de la Recherche, ANR-13-JS09-0004-01 (STRATIMIX). Data use requests can be directed to hans.van.haren@nioz.nl.

The Editor thanks two anonymous reviewers for their assistance in evaluating this paper.

References

Bacmeister, J. T., and M. R. Schoeberl (1989), Breakdown of vertically propagating two-dimensional gravity waves forced by orographym, *J. Atmos. Sci.*, *46*, 2109–2134.

Corcos, G. M., and F. S. Sherman (1976), Vorticity concentration and the dynamics of unstable free shear layers, *J. Fluid Mech.*, *73*, 241–264.

Dillon, T. M. (1982), Vertical overturns: A comparison of Thorpe and Ozmidov length scales, *J. Geophys. Res.*, *87*, 9601–9613, doi:10.1029/JC087iC12p09601.

Farmer, D., and L. Armi (1999), Stratified flow over topography: The role of small-scale entrainment and mixing in flow establishment, *Proc. R. Soc. London A*, *455*, 3221–3258.

Ferron, B., et al. (1998), Mixing in the Romanche Fracture Zone, *J. Phys. Oceanogr.*, *28*, 1929–1945.

Fukao, S., H. Luce, T. Mega, and M. K. Yamamoto (2011), Extensive studies of large-amplitude Kelvin-Helmholtz billows in the lower atmosphere with VHF middle and upper atmosphere radar, *Q. J. R. Meteorol. Soc.*, *137*, 1019–1041, doi:10.1002/qj.807.

Geyer, W. R., and J. D. Smith (1987), Shear instability in a highly stratified estuary, *J. Phys. Oceanogr.*, *17*, 1668–1679.

Geyer, W. R., A. C. Lavery, M. E. Scully, and J. H. Trowbridge (2010), Mixing by shear instability at high Reynolds number, *Geophys. Res. Lett.*, *37*, L22607, doi:10.1029/2010GL045272.

Gregg, M. C. (1989), Scaling turbulent dissipation in the thermocline, *J. Geophys. Res.*, *94*, 9686–9698, doi:10.1029/JC094iC07p09686.
Howard, L. N. (1961), Note on a paper of John W. Miles, *J. Fluid Mech.*, *10*, 509–512.
Mantyla, A. W., and J. L. Reid (1983), Abyssal characteristics of the World Ocean waters, *Deep Sea Res.*, *30*, 805–833.
Mashayek, A., C. P. Caulfield, and W. R. Peltier (2013), Time-dependent, non-monotonic mixing in stratified turbulent shear flows: Implications for oceanographic estimates of buoyancy flux, *J. Fluid Mech.*, *736*, 570–593, doi:10.1017/jfm.2013.551.
McDougall, T. J., et al. (2009), *Calculation of the Thermodynamic Properties of Seawater, Global Ship-Based Repeat Hydrography Manual, IOCCP Rep. 14*, *ICPO Publ. Ser., 134*, U.N.E.S.C.O, Paris.
Mercier, H., and P. Morin (1997), Hydrography of the Romanche and Chain Fracture Zones, *J. Geophys. Res.*, *102*, 10,373–10,389, doi:10.1029/97JC00229.
Mercier, H., and K. G. Speer (1998), Transport of bottom water in the Romanche Fracture Zone and the Chain Fracture Zone, *J. Phys. Oceanogr.*, *28*, 779–790.
Miles, J. W. (1961), On the stability of heterogeneous shear flows, *J. Fluid Mech.*, *10*, 496–508.
Morozov, E., A. Demidov, R. Tarakanov, and W. Zenk (2010), *Abyssal Channels in the Atlantic Ocean: Water Structure and Flows*, 266 pp., Springer, Heidelberg.
Munk, W., and C. Wunsch (1998), Abyssal recipes II: Energetics of tidal and wind mixing, *Deep Sea Res., Part I*, *45*, 1977–2010.
Osborn, T. R. (1980), Estimates of the local rate of vertical diffusion from dissipation measurements, *J. Phys. Oceanogr.*, *10*, 83–89.
Polzin, K. L., K. G. Speer, J. M. Toole, and R. W. Schmitt (1996), Intense mixing of Antarctic bottom water in the equatorial Atlantic Ocean, *Nature*, *380*, 54–57.
Scinocca, J. F., and R. Ford (2000), The nonlinear forcing of large-scale internal gravity waves by stratified shear instability, *J. Atmos. Sci.*, *57*, 653–672.
Smith, W. H. F., and D. T. Sandwell (1997), Global seafloor topography from satellite altimetry and ship depth soundings, *Science*, *277*, 1957–1962.
Smyth, W. D., and J. N. Moum (2012), Ocean mixing by Kelvin-Helmholtz instability, *Oceanography*, *25*, 140–149, doi:10.5670/oceanog.2012.49.
Smyth, W. D., and J. N. Moum (2013), Marginal instability and deep cycle turbulence in the eastern equatorial Pacific Ocean, *Geophys. Res. Lett.*, *40*, 6181–6185, doi:10.1002/2013GL058403.
Tarakanov, R. Y., N. I. Makarenko, and E. G. Morozov (2013), Antarctic bottom water flow in the western part of the Romanche Fracture Zone based on the measurements in October of 2011, *Oceanology*, *53*, 655–667, doi:10.1134/S0001437013050147.
Thorpe, S. A. (1968), A method of producing a shear flow in a stratified fluid, *J. Fluid Mech.*, *32*, 693–704.
Thorpe, S. A. (1977), Turbulence and mixing in a Scottish loch, *Philos. Trans. R. Soc. London*, *286*, 125–181.
Thorpe, S. A. (2005), *The Turbulent Ocean*, 439 pp., Cambridge Univ. Press, Cambridge, U. K.
van Haren, H., and L. Gostiaux (2012), Detailed internal wave mixing observed above a deep-ocean slope, *J. Mar. Res.*, *70*, 173–197, doi:10.1357/002224012800502363.
van Haren, H., et al. (1999), Strong inertial currents and marginal internal wave stability in the central North Sea, *Geophys. Res. Lett.*, *26*, 2993–2996, doi:10.1029/1999GL002352.
van Haren, H., et al. (2009), NIOZ3: Independent temperature sensors sampling yearlong data at a rate of 1 Hz, *IEEE J. Ocean. Eng.*, *34*, 315–322, doi:10.1109/JOE.2009.2021237.
Wesson, J. C., and M. C. Gregg (1994), Mixing at camarinal sill in the strait of gibraltar, *J. Geophys. Res.*, *99*, 9847–9878, doi:10.1029/94JC00256.